Supporting Information

Moeller et al. 10.1073/pnas.1700122114

SI Materials and Methods

Sample Collection and Processing. Carnivore and artiodactyl samples were located by scat-detection dogs as described previously (46, 47). Carnivore and artiodactyl samples were collected across an ∼300-square-mile region in northeast Washington State. Only visibly moist samples were collected to minimize environmental contamination and sample degradation. The large size of the study area was intended to minimize the probability of sampling individual hosts multiple times. Samples were frozen 3–8 h after collection and subsequently were stored at −80 °C. For the carnivore and artiodactyl samples, the core of each fecal pellet was subsampled before DNA extraction. Rodent samples were collected directly from captured animals, transferred to RNAlater (Ambion), and subsequently frozen and stored at −80 °C.

Statistical Analyses. Geographic distances between sampling locations were retrieved from Google Earth. To model the exponential decay of compositional overlap (i.e., 1 − Bray–Curtis dissimilarity) between host-species microbiotas over evolutionary time and across geographic space, nonlinear least squares regressions were performed with the stats package in **R**.

Statistical significance of associations between compositional overlap and evolutionary distances was assessed through Mantel tests, as implemented in the vegan package in **R**. To examine the effects of geographic distance and phylogenetic divergence on gut-microbiota β-diversity between host populations, linear models were constructed, and likelihood ratio tests were performed in **R** using the lmtest package. Variance partitioning was performed with the vegan package in **R**. Significant differences between mean Bray–Curtis dissimilarities calculated from pairwise comparisons of the gut microbiotas of host species were assessed through nonparametric P values generated by 1,000 Monte Carlo permutations as implemented in make_distance_comparison_plots.py in QIIME. A dendrogram of all samples was produced via upgma_cluster.py in QIIME.

SI Results

Geographic Distance Promotes Divergence Between the Gut Microbiotas of Allopatric Host Populations. To further assess whether geographic distances and divergence times between host populations were each independently associated with compositional differences between the gut microbiotas of host populations, we performed variance partitioning analysis in **R** via the vegan package. This analysis indicated that 3.1% of the variance in compositional overlap between the microbiotas of allopatric host populations could be explained by geographic distances between host populations independently of host phylogenetic divergences, whereas 49.1% could be explained by host phylogenetic divergences independently of geographic distances between host populations. However, we note that the variance explained by these two variables depends heavily on the details of sampling (for example, 8 of 17 host species were sampled in a single geographic region) and does not necessarily reflect estimates of the relative effect sizes of geographic distance and phylogenetic divergence on gut microbiota divergence between host species. Instead, these results indicate that compositional overlap between the microbiotas of host species is negatively influenced by the geographic distance separating the hosts in addition to host phylogenetic divergence. This result is further supported by likelihood ratio tests that revealed that compositional overlap was better modeled as a linear combination of host divergence times and geographic distances between host populations than as linear functions containing only host divergence times ($P = 0.0488$) or only geographic distances between host populations ($P < 2.2 \times 10^{-16}$).

Similarity of Predator and Prey Microbiotas Is Not Due to Parallel Acquisition of Environmental Bacteria. One possible explanation for the convergence of predator and prey gut microbiotas is that predators and prey display more similar preferences for microhabitats within their shared environments than do predators and nonprey, leading predators and prey to acquire more similar sets of environmental bacteria. However, this explanation is less likely than the transfer of bacteria between predators and prey because all the predator species in our dataset are wide-ranging and experience many of the same microhabitats (55). Moreover, many of the phylotypes that display signatures of transfer belong to genera of bacterial symbionts (e.g., *Helicobacter* and *Bifidobacterium*) (Dataset S4). In fact, 323 of the 419 phylotypes that displayed signatures of transfer belonged to the Firmicutes or the Bacteroidetes, the two most dominant phyla in the mammalian gut, and all these phylotypes could be further classified to subphyla taxonomic groups known to inhabit mammals (Dataset S4). Similarly, the putatively transferred phylotypes belonging to phyla other than the Firmicutes or Bacteroidetes were readily classified to genera/families known to inhabit mammals. For example, 75% of the phylotypes belonging to the phylum Actinobacteria were classified to the genus *Bifidobacterium*, a genus of symbionts specialized to the gut. These results suggest that the compositional convergence of predator and prey gut microbiotas is due primarily to the transfer of gut bacteria between hosts and not to the parallel acquisition of environmental bacteria from sources private to predators and their prey.

Convergence of Predator and Prey Microbiotas Cannot Be Explained by Host Body Size. The apparent effects of predator–prey relationships on gut-microbiota composition are confounded with differences in body size among hosts, i.e., smaller and larger carnivore species prefer smaller and larger prey species, respectively. To explore whether the convergence of the gut microbiotas of predators and prey can be explained by host body-size effects, we tested whether the gut microbiotas of large-bodied carnivores (i.e., *Canis lupus* and *Puma*) were compositionally more similar to those of large-bodied *Rangifer*, whose species range does not overlap with the sampling region in northeast Washington State and on which these carnivores do not prey, than were the microbiotas of small-bodied carnivores (i.e., *Canis latrans* and *Lynx*). In contrast to the pattern observed for predator–prey species pairs, the gut microbiotas of *Canis lupus* were compositionally less similar to those of allopatric *Rangifer* than were the microbiotas of *Canis latrans* (nonparametric $P = 0.001$) (Fig. S2 and Dataset S2). Similarly, in several cases the gut microbiotas of small-bodied carnivores were compositionally less similar to those of allopatric populations of rodent species whose ranges do not coincide with the sampling region in northeast Washington State than were the gut microbiotas of large-bodied carnivores (Dataset S2). For example, the gut microbiotas of *Canis latrans* were less compositionally similar on average to those of *Onychomys* than were the gut microbiotas of *Canis lupus* (nonparametric $P = 0.001$) (Dataset S2). In addition, the gut microbiotas of small-bodied carnivores were compositionally more similar to those of allopatric populations of rodent species whose species ranges coincide with the sampling region in northeast Washington (i.e., *Peromyscus*, *Perognathus*,

Tamias, and *Sciurus*) than to those of allopatric rodent populations whose species ranges do not coincide with the ranges of the carnivores (nonparametric $P = 0.001$) (Dataset S2). These results suggest that the gut microbiotas of predators and their prey have converged due to predator–prey interactions and not body-size effects.

Co-occurrence of Phylotypes from Multiple Prey Species Within Individual Carnivore Fecal Samples. One explanation for the compositional convergence between predator and prey gut microbiotas is the transient passage of prey-derived bacteria through carnivore gastrointestinal tracts following feeding events. We reasoned that the co-occurrence of bacterial phylotypes derived from multiple prey species within individual carnivore fecal samples would indicate that prey-derived bacterial phylotypes persist and proliferate within individual carnivores. To test whether individual carnivore fecal samples harbored bacterial phylotypes derived from multiple prey species, we identified all bacterial phylotypes shared by *Lynx*, *Canis latrans*, and precisely one small-bodied prey species (i.e., *Tamias*, *Perognathus*, *Peromyscus*, or *Sciurus*) but not by *Puma* and *Canis lupus*. In addition, we identified all bacterial phylotypes shared by *Puma*, *Canis lupus*, and precisely one large-bodied prey species (i.e., *Alces*, *Odocoileus*, or *Cervus*) but not by *Lynx* and *Canis latrans*. The abundances of these phylotypes across carnivore samples are presented in Dataset S5. Consistent with the persistence and proliferation of prey-derived phylotypes within carnivores, the majority of individual carnivore fecal samples contained bacterial phylotypes derived from multiple prey species.

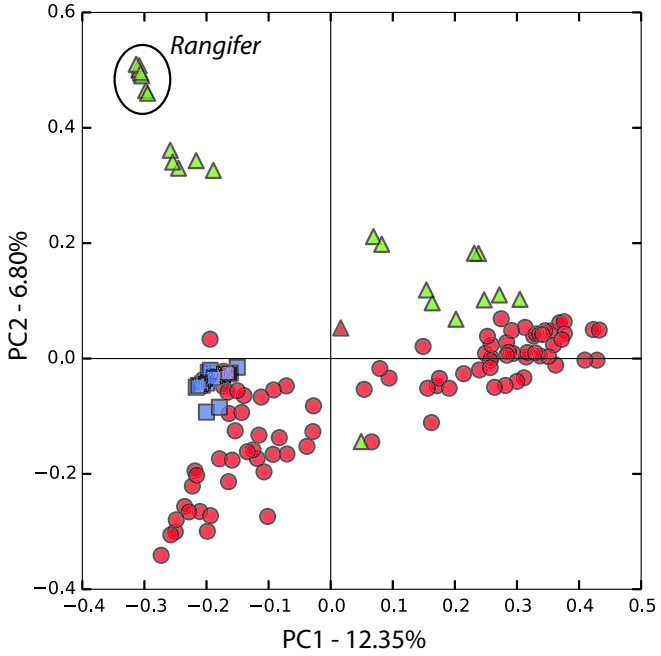

Fig. S1. Variation in microbiota composition across mammalian orders. Principal coordinates (PC1 and PC2) plots of the Bray–Curtis dissimilarities among fecal samples collected from three mammalian orders. Samples collected from Carnivora, Artiodactyla, and Rodentia are represented by red circles, light-green triangles, and blue squares, respectively. Samples collected from *Rangifer* living allopatrically from the sampled carnivores are circled.

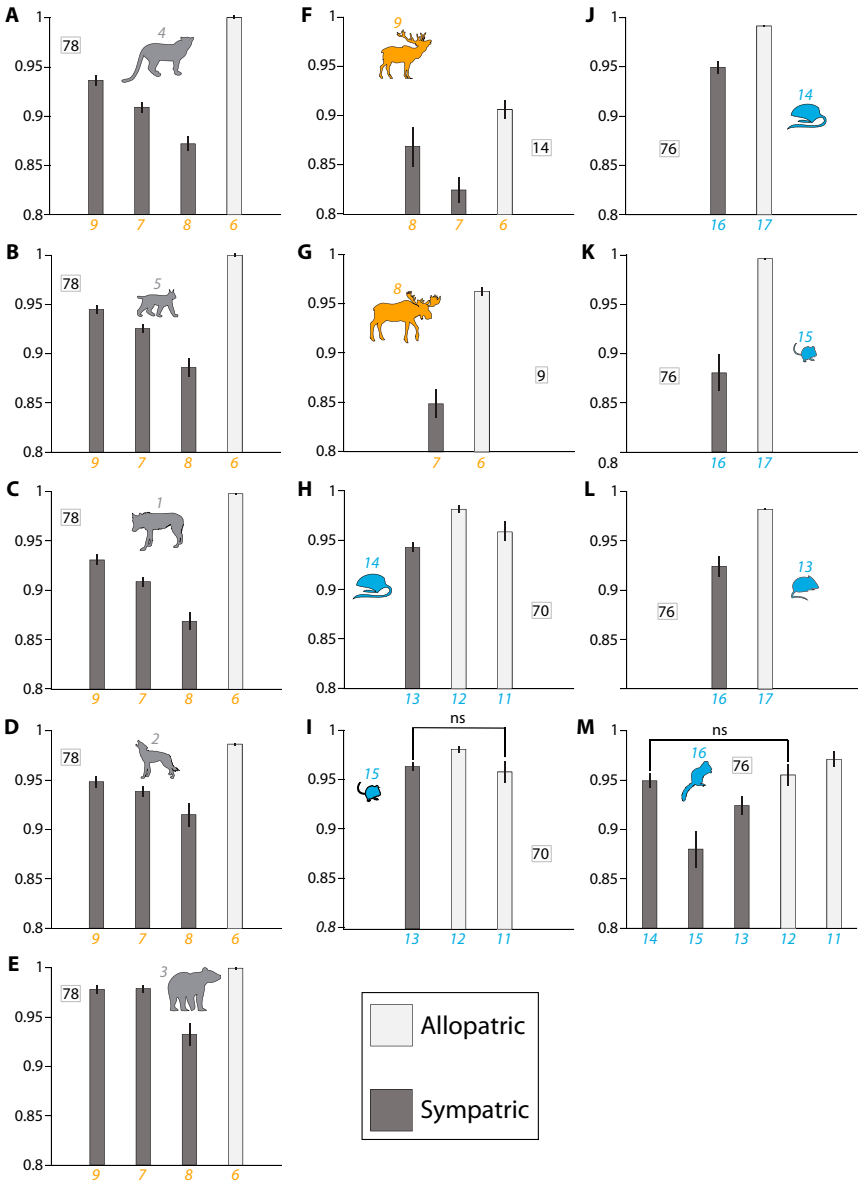

Fig. S2. Convergence of the gut microbiotas of sympatric populations of host species. Each panel displays the mean Bray–Curtis dissimilarity between the gut microbiotas of a focal host population (denoted by a colored cartoon and a colored number corresponding to Fig. 1) and the gut microbiotas of sympatric and allopatric host populations (denoted by colored numbers along the *x* axis) of a specific phylogenetic divergence from the focal host population. Focal host populations in *A*–*M* are *Puma concolor* (*A*), *Lynx rufus* (*B*), *Canis lupus* (*C*), *Canis latrans* (*D*), *Ursus arctos* (*E*), *Cervus elaphus* (*F*), *Alces alces* (*G*), *Dipodomys ordii* (*H*), *Perognathus parvus* (*I*) *Dipodomys ordii* (*J*), *Perognathus parvus* (*K*), *Peromyscus maniculatus* (*L*), and *Tamius minimus* (*M*). In each panel, the number within the box denotes the divergence time in millions of years of the focal host population from the other host populations. The gut microbiotas of allopatric host populations were always significantly more compositionally divergent from the gut microbiotas of the focal host population than were the gut microbiotas of sympatric host populations ($P = 0.001$; nonparametric tests based on Monte Carlo permutations), except in two cases marked as not significant (ns).

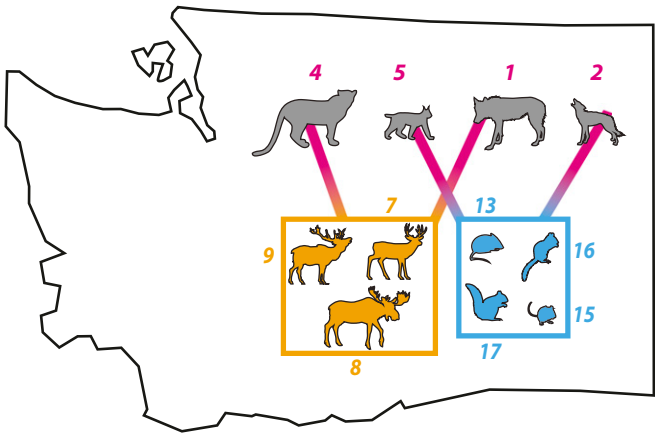

Fig. S3. Prey preferences of mammalian carnivores. Boxes contain prey whose species ranges overlap with the sampling region in northeast Washington State. Numbers correspond to host-species labels in Fig. 1. Colored bars connecting individual predator species with sets of prey species indicate preference by predators for specific orders of prey.

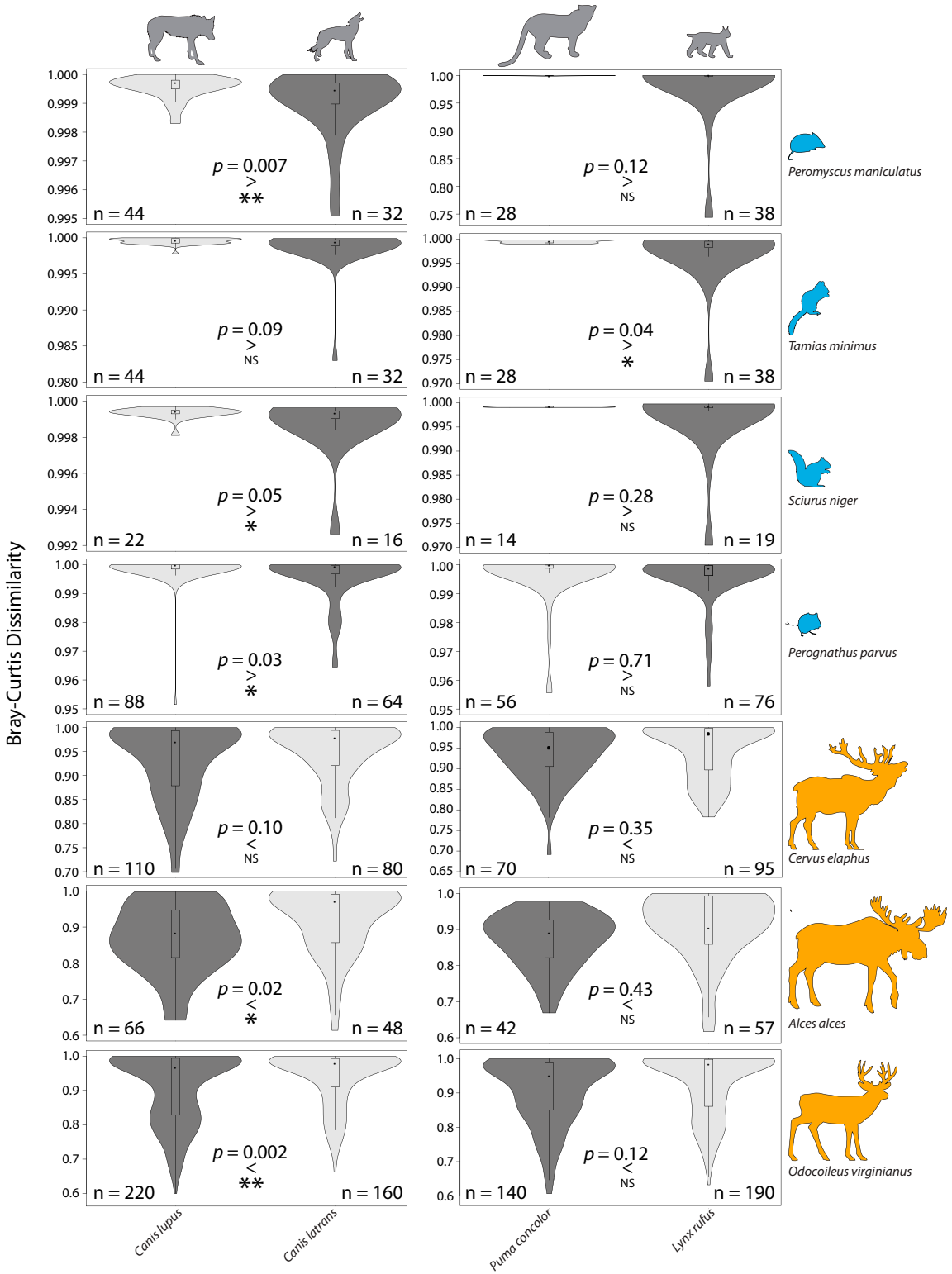

Fig. S4. Predators and their preferred prey harbor compositionally similar gut microbiotas. Violin plots show the distributions of Bray–Curtis dissimilarities between the microbiotas of predator and prey host populations. Each box displays two pairwise comparisons between predator populations (columns) and prey populations (rows). Each violin plot displays the kernel density estimation of Bray–Curtis dissimilarities, such that the width of the plots indicates the proportion of Bray–Curtis dissimilarities at different *y*-axis values. Colors of cartoons correspond to host taxonomic orders as in Fig. 1. Black dots within box-and-whisker plots represent means. Within each box, the direction of the difference between mean Bray–Curtis dissimilarities is denoted by a greater-than (>) or less-than (<) symbol, and violin plots with higher and lower mean Bray–Curtis dissimilarities are colored in light and dark gray, respectively. The significance of differences between means, based on Bonferroni-corrected *P* values, is denoted as not significant (ns), $*P < 0.05$, and $**P < 0.01$. Bonferroni-corrected *P* values for each test and the number of pairwise comparisons represented by each violin are shown.

Fig. S5. Convergence of the gut microbiotas of individual predators and prey. Dendrogram of Bray–Curtis dissimilarities among mammalian microbiotas visualized by unweighted pair group method with arithmetic mean (UPGMA) clustering. Each terminal branch represents the microbiota of an individual fecal sample. Branches are colored by host order as in Fig. 1.

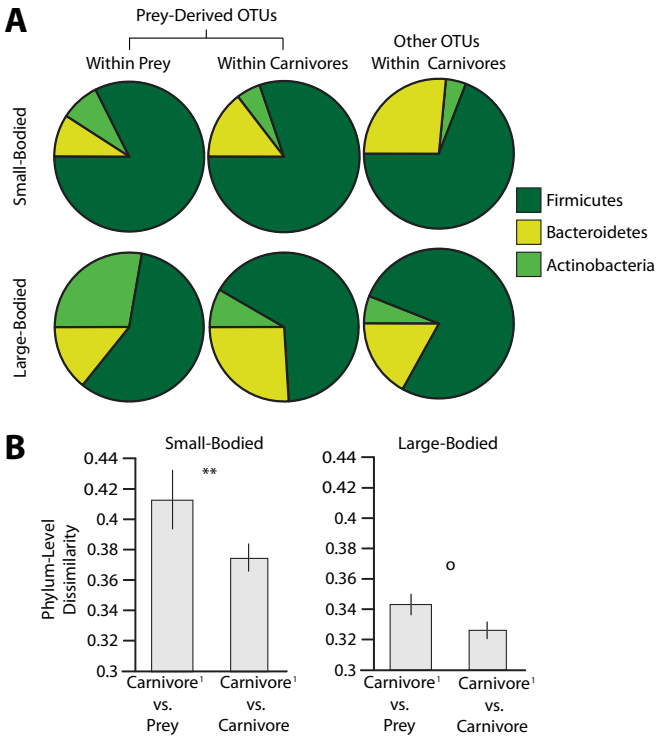

Fig. S6. Relative abundances of prey-derived phylotypes in carnivores resemble a carnivore-like phylum-level profile. (*A*) Pie charts display relative abundances of putatively prey-derived OTUs belonging to the Firmicutes, Bacteroidetes, and Actinobacteria within prey (*Left*) and carnivores (*Center*) as well as the relative abundances of non–prey-derived OTUs belonging to the Firmicutes, Bacteroidetes, and Actinobacteria within carnivores (*Right*). (*B*) Bray–Curtis dissimilarities between phylum-level compositional profiles of putatively prey-derived OTUs within carnivores (Carnivore[1]) and phylum-level compositional profiles of other OTUs within carnivores and prey. Significant differences were assessed by nonparametric *P* values generated by Monte Carlo permutations: o, $P < 0.1$; **$P < 0.01$.

Table S1. Species for which fecal samples were collected and sample counts

Common name	Binomial name	No. of samples
Black bear	*Ursus americanus*	23
Coyote	*Canis latrans*	34
Wolf	*Canis lupus*	27
Bobcat	*Lynx rufus*	25
Mountain lion	*Puma concolor*	17
Great Basin pocket mouse	*Perognathus parvus*	6
Ord's kangaroo rat	*Dipodomys ordii*	7
Fox squirrel	*Sciurus niger*	1
Least chipmunk	*Tamias minimus*	2
Deer mouse	*Peromyscus maniculatus*	9
Northern grasshopper mouse	*Onychomys leucogaster*	3
California vole	*Microtus californicus*	6
Tuco-tuco	*Ctenomys cf knightii*	13
Caribou	*Rangifer tarandus*	10
White-tailed deer	*Odocoileus virginianus*	11
Moose	*Alces alces*	4
Elk	*Cervus elaphus*	6

Dataset S1. List of samples and their corresponding metadata

Dataset S1

Dataset S2. Mean Bray–Curtis dissimilarities for all pairwise comparisons between the gut microbiotas of mammal species

Dataset S2

Dataset S3. Taxonomic assignments and relative abundances of bacterial phylotypes displaying geographic specificity

Dataset S3

Dataset S4. Taxonomic assignments and relative abundances of bacterial phylotypes underlying the convergence of predator and prey microbiotas

Dataset S4

Species designations for each sample are presented in Table S1.

Dataset S5. Taxonomic assignments and relative abundances of bacterial phylotypes shared by carnivores and precisely one prey species

Dataset S5

Species designations for each sample are presented in Table S1.

Dataset S6. Taxonomic assignments of phylotypes based on SILVA

Dataset S6